

# The industrial glass melting process

Reinhard Conradt

RWTH Aachen, Institut für Gesteinshüttenkunde und  
Lehrstuhl für Glas und keramische Verbundwerkstoffe, Mauerstr. 5, 52064 Aachen

## 1. Introduction to some fundamentals of industrial glass melting

The present article gives an example of the application of thermodynamic data to a quite complex technical process, i.e., the industrial melting of glass.

The glass melting process starts from a granular mixture of natural and synthetic raw materials (the so-called batch) and yields a thermally and chemically homogeneous melt made available at a well defined temperature level. The consecutive steps of glass fabrication (forming, annealing, etc.) are not within the scope of interest of this paper. Figure 1 illustrates how a continuously working glass melting furnace functions in principle. Figure 2 presents in very general terms a heat balance of the glass melting process. It comprises amounts of heat related to the flow of matter led through the combustion space, amounts of heat related to the flow of matter led through the melting basin, and heat losses through the boundaries of the system. For simplicity, all quantities are referred to the standard temperature level  $T_0 = 298$  K of the environment and to isobaric conditions at  $p = 1$  bar. The quantity of specific interest in this paper is the so-called exploited heat  $H_{ex}$ . It comprises both the heat required to bring about the batch-to-melt conversion, and the heat stored in the homogeneous melt leaving the system boundary at a temperature  $T_{ex}$ . For the quantification of the heat balance in figure 2, it is crucial to have an accurate account of  $H_{ex}$ . It is true, the contributions  $H_{in}$ ,  $H_{off}$ ,  $H_{stack}$ , and  $H_{re}$  related to the combustion space can be calculated in a most accurate way from measured process temperatures, and from the known amounts of fuel and air used. But for the wall losses  $H_{wo}$  and  $H_{wu}$  through the boundaries of the combustion space and the basin, respectively, rough estimates are available only. This is due to the complicated shape of a real glass furnace, to the presence of a considerable number of openings in the furnace walls, and – most of all, after some years of continuous furnace operation – to the unknown residual thickness of the refractory bricks of the furnace lining. Thus, if  $H_{ex}$  is assessed at a high accuracy, then the balance in figure 2 can be completed, and even an accurate account of the wall losses may be obtained.

As stated above, the exploited heat  $H_{ex}$  comprises both the heat required for the batch-to-melt conversion and the heat physically stored in the homogeneous melt at  $T = T_{ex}$ . Irrespective of the actual reaction path leading from the batch at  $T_0$  to the melt at  $T_{ex}$ ,  $H_{ex}$  may be presented as

$$H_{ex} = \Delta H_{chem}^{\circ} + \Delta H_{melt}(T_{ex}), \quad (1)$$

where  $\Delta H_{chem}^{\circ}$  denotes the enthalpy difference at  $T = 298$  K between the batch on one side, and the glass plus the gases released from the batch on the other side,

$$\text{batch (298 K)} \rightarrow \text{glass (298 K)} + \text{batch gases (298 K)}, \quad (2)$$

and  $\Delta H_{\text{melt}}(T_{\text{ex}})$  denotes the enthalpy difference between the glass at 298 K and the glass melt at  $T = T_{\text{ex}}$ . This approach to  $H_{\text{ex}}$  comprises a dual challenge: We need an accurate approach to the thermodynamics of multicomponent glasses at room temperature, and to multicomponent melts.

## 2. Description frame for the thermodynamic properties of industrial glass-forming-systems

### 2.1 Description frame for one-component glasses and glass melts

The thermodynamic state of a one-component system in its stable liquid, metastable undercooled, glassy, and crystalline state at an ambient pressure of  $p = 1$  bar is described by the following seven quantities in a comprehensive way. These are:

- $H^\circ$  = the standard enthalpy at 298 K, for the crystalline solid, stable at  $T = T_g$ ,
- $S^\circ$  = the standard entropy at 298 K, for the crystalline solid, stable at  $T = T_g$ ,
- $H^{\text{fus}}$  = the enthalpy of fusion,
- $T_{\text{liq}}$  = the liquidus temperature,
- $c_P(T)$  = the heat capacity of the crystalline solid as a function of temperature as, e.g., represented by the polynomial  $c_P(T) = A + B \cdot T + C/T^2$ ,
- $H^{\text{vit}}$  = the vitrification enthalpy,
- $S^{\text{vit}}$  = the vitrification entropy (zero Kelvin entropy of the glass),
- $\Delta c_P$  = the jump of the heat capacity at the glass transition temperature,
- $T_g$  = the glass transition temperature.

In principle, all quantities referring to the glassy state depend on the cooling rate at which this state is reached. With the cooling rate defined, they assume unambiguous values. The details are not elaborated here. The set of quantities  $H^{\text{fus}}$ ,  $S^{\text{fus}}$ ,  $T_{\text{liq}}$ ,  $H^{\text{vit}}$ ,  $S^{\text{vit}}$ ,  $\Delta c_P$ , and  $T_g$  is redundant. It is linked by the relations given in eqs. 3 to 5 a-c.  $H_c(T)$  and  $S_c(T)$  denote the configurational enthalpy and entropy, respectively.

$$S^{\text{fus}} = H^{\text{fus}} / T_{\text{liq}} \quad (3)$$

$$H_c(T) = H^{\text{vit}} + \int_{T_g}^T (c_{P,\text{liq}} - c_{P,\text{cryst}}) dT = H^{\text{fus}} - \int_T^{T_{\text{liq}}} (c_{P,\text{liq}} - c_{P,\text{cryst}}) dT \quad (4a)$$

$$\approx H^{\text{vit}} + ? c_P \cdot (T - T_g) \approx H^{\text{fus}} - ? c_P \cdot (T_{\text{liq}} - T) \quad (4b)$$

$$H^{\text{vit}} \approx H^{\text{fus}} - ? c_P \cdot (T_{\text{liq}} - T_g) \quad (4c)$$

and

$$S_C(T) = S^{vit} + \int_{T_g}^T \frac{c_{P,liq} - c_{P,cryst}}{T} dT = S^{fus} - \int_T^{T_{liq}} \frac{c_{P,liq} - c_{P,cryst}}{T} dT \quad (5a)$$

$$\approx S^{vit} - \int_{T_g}^T c_p \cdot \ln \frac{T}{T_g} \approx S^{fus} - \int_T^{T_{liq}} c_p \cdot \ln \frac{T}{T_{liq}} \quad (5b)$$

$$S^{vit} \approx S^{fus} - \int_{T_g}^{T_{liq}} c_p \cdot \ln \frac{T}{T_g} \quad (5c)$$

The knowledge of any four of the above redundant set of quantities is sufficient to derive the rest. As shown by a large number of calorimetric experiments [1], the error introduced by the approximation of the real shape of the  $\Delta c_p$  jump by a constant value is calorimetrically insignificant. Thus  $H_C(T)$  and  $S_C(T)$  may be calculated as suggested by eqs. 4 c and 5 c.

## 2.2 Description frame for multi-component glasses and glass melts

The thermodynamic properties of multi-component systems have been approached by different elaborate models, among which are: the (modified) quasi-chemical model [2], the cell model [3], the model of ideal mixing of complex components [4-5]. But even for elaborate computer codes and databases used in computational thermochemistry [6-7], the generation of reliable data for multi-component systems still is a major problem. The author's own approach [8-10] outlined below is especially well suited for the multi-component systems typical of industrial glasses:

The rigid glass as well as the glass melt are described by their energetic and entropic difference to a normative state of mineral phases  $k$  which would form and coexists at the glass transition temperature  $T_g$  under equilibrium conditions. This state has been termed "crystalline reference system" (c.r.s.). In the temperature interval from absolute zero to  $T_g$ , the rigid glass differs from the c.r.s. by an enthalpy and entropy of vitrification,  $H^{vit}$  and  $S^{vit}$ , respectively. In the same way, the melt at liquidus temperature  $T_{liq}$  differs by an enthalpy and entropy of fusion:  $H^{fus}$  and  $S^{fus}$ . The glass and the melt are regarded as a mixture of glassy and melted compounds  $k$ , respectively. Heats (enthalpies) and entropies of mixing, which usually make very large contributions in silicate systems if referred to the oxide components  $j$ , become negligibly small if referred to the c.r.s. compounds  $k$ . The crucial step is the identification of the appropriate set of compounds  $k$ . An adequate strategy is developed by exploiting two fundamental principles found to be valid in the mineral world. These are:

- *the principle of majority partition.*

By experience, even complicated multi-component systems, such as magmatic and igneous rock melts, metallurgical slags, commercial glasses, etc., can be represented by a predominant quaternary typically comprising more than 85 – 95 % of the oxides on a molar basis.

- *the principle of parsimony.*

The very large number of combinatorial possibilities of compound formation is not exploited by nature. Rather, a quite limited set of binary and ternary compounds is

found. The constitutional relations in a given multi-component system are therefore approximated in the following way: First, the minority oxides are allotted to a set of normative phases as suggested by the CIPW norm calculation (see e.g. [11]). The remaining four majority oxides are allotted to the respective constitutional sub-range in the predominant quaternary identified and reconstructed by the evaluation of existing phase diagrams. The details are described in [10].

According to Gibbs' phase rule, the number of oxides  $j$  in a glass composition is identical to the number of compounds  $k$  in the corresponding c.r.s.; the molar amounts  $n$  or masses  $m$  of the  $j$  and  $k$  (given in kmol or kg, respectively, per 100 kg of glass) are thus related by a linear equation system,

$$\bar{n}_j = (v_{jk}) \cdot \bar{n}_k \Rightarrow \bar{n}_k = (B_{kj}) \cdot \bar{n} \quad , \quad (6 \text{ a})$$

$$\bar{m}_j = (\mu_{jk}) \cdot \bar{m}_k \Rightarrow \bar{m}_k = (A_{kj}) \cdot \bar{m}_j \quad , \quad (6 \text{ b})$$

$$(A_{kj}) = (v_{jk})^{-1}, (B_{kj}) = (\mu_{jk})^{-1} \quad . \quad (6 \text{ c})$$

Here,  $v_{jk}$  is the matrix element telling how many mol of oxide  $j$  are found in compound  $k$ ;  $\mu_{jk}$  tells how many kg of oxide  $j$  are contained in 1 kg of compound  $k$ .  $A_{kj}$  and  $B_{kj}$  are the elements of the inverted matrices  $(v_{jk})$  and  $(\mu_{jk})$ , respectively. As an example, table 1 presents the main oxides  $j$  and compounds  $k$ , and the matrix elements  $B_{kj}$  used for E glass compositions. The composition of an E glass depicted as example and reference [12] is shown in table 2 in terms of both oxides  $j$  and compounds  $k$ .

The thermodynamic quantities of a glass or its melt are obtained by the following set of equations (7 a-g):

$$H_{\text{glass}}^{\circ} = \sum_k n_k \cdot (H_k^{\circ} + H_k^{\text{vit}}) \quad , \quad (7 \text{ a})$$

$$H_{1673,\text{melt}}^{\circ} = \sum_k n_k \cdot H_{1673,\text{melt},k}^{\circ} \quad , \quad (7 \text{ b})$$

$$S_{\text{glass}}^{\circ} = \sum_k n_k \cdot (S_k^{\circ} + S_k^{\text{vit}}) \quad , \quad (7 \text{ c})$$

$$S_{1673,\text{melt}}^{\circ} = \sum_k n_k \cdot S_{1673,\text{melt},k}^{\circ} \quad , \quad (7 \text{ d})$$

$$c_{P,\text{melt}} = \sum_k n_k \cdot c_{P,\text{melt},k} \quad , \quad (7 \text{ e})$$

$$H_{T,\text{melt}} = H_{1673,\text{melt}}^{\circ} + c_{P,\text{melt}} \cdot (T - 1673) \quad , \quad (7 \text{ f})$$

$$S_{T,\text{melt}} = S_{1673,\text{melt}}^{\circ} + c_{P,\text{melt}} \cdot \ln(T/1673) \quad . \quad (7 \text{ g})$$

$H_{\text{glass}}^{\circ}$  is the standard enthalpy (heat) of the rigid glass (at 25 °C, 1 bar),  $H_{1673,\text{liq}}^{\circ}$  is the heat of the melt at 1400 °C (= 1673.15 K);  $H_{T,\text{liq}}$  is the heat of the melt at arbitrary temperature  $T$ ; entropies  $S$  have the analogous meaning;  $c_{P,\text{liq}}$  is the heat capacity of the melt above  $T_{\text{liq}}$ . The quantities of the individual compounds  $k$  used in eqs. (7 a-g) are compiled in table 3. This table does not only allow to calculate the properties of E glasses, but also of A fibre, C fibre, stone and slag wool, crystal, low-expansion, container, and float glasses. For an appropriate determination of the c.r.s. of the different types of industrial glasses, please consult [10].

The following data give an impression of the accuracy of the approach: Gibbs energies of formation were calculated for four different mineral wool glasses. The values were checked by calorimetry by an independent laboratory [13], yielding the following experimental vs. calculated values for the standard Gibbs energies of formation from the elements (in kJ per mol of oxides): -852.0 vs. -849.6; -865.0 vs. -867.2; -880.8 vs. -881.8; -855.4 vs. -852.7. The standard Gibbs energies of formation from the oxides read: -12.9 vs. -10.6; -35.4 vs. -37.7; -34.0 vs. -35.0; -44.1 vs. -41.4.

### 2.3 Heat Content of Glass Melts

For our reference E glass (see table 2), the following results are obtained:

$$\begin{aligned}
 H^\circ &= -15,112 \text{ kJ/kg} &= -4,197.8 \text{ kWh/t}, \\
 H^{\text{vit}} &= 291 \text{ kJ/kg} &= 80.9 \text{ kWh/t}, \\
 H^\circ_{\text{glass}} &= -14,821 \text{ kJ/kg} &= -4,116.9 \text{ kWh/t}, \\
 H_{1673,\text{liq}} &= -13,039 \text{ kJ/kg} &= -3,621.8 \text{ kWh/t}, \\
 C_{P,\text{liq}} &= 1,454 \text{ J/(kg}\cdot\text{K)} &= 404.0 \text{ Wh/(t}\cdot\text{K)}, \\
 S^{\text{vit}} &= 135 \text{ J/(kg}\cdot\text{K)} &= 37.6 \text{ Wh/(t}\cdot\text{K)},
 \end{aligned}$$

All quantities are given in S.I. units J, kg, K. In order to allow an easy comparison to electrical energy, the quantities are also given in kWh/t and Wh/(t·K) for heats and entropies, respectively; 1 t = 1,000 kg. From the above data, a number of data with high practical importance are derived. As an immediate example, the heat content of a given glass melt (relative to 25 °C) at arbitrary temperature T is given by

$$\Delta H_{T,\text{melt}} = H_{T,\text{melt}} - H^\circ_{\text{glass}} \quad (8)$$

For our reference E glass, the following results are obtained:

$$\begin{aligned}
 \Delta H_{T,\text{liq}} &= 1,782 \text{ kJ/kg} = 495.0 \text{ kWh/t for } 25 - 1400 \text{ }^\circ\text{C}, \\
 &= 1,636 \text{ kJ/kg} = 454.6 \text{ kWh/t for } 25 - 1300 \text{ }^\circ\text{C}.
 \end{aligned}$$

For a glass melting process with a pull temperature  $T_{\text{ex}} = 1300 \text{ }^\circ\text{C}$ , the last line represents the value  $\Delta H_{\text{melt}}(T_{\text{ex}})$  in eq. (1). Thus, an essential part in determining  $H_{\text{ex}}$  has been accomplished. What is left is the determination of the chemical term  $\Delta H^\circ_{\text{chem}}$ .

An additional comment: It is true, the heat content of a melt may also be estimated from existing oxide increment systems [14-16]. As shown in table 4 for the example of a mineral fibre glass, however, the direct thermodynamic approach is more accurate. Since the increment systems are based on a quite restricted composition range only, the thermodynamic approach is also more versatile compositionally.

## 3. The batch-to-melt conversion

### 3.1 Heat demand of the batch-to-melt conversion, simple raw materials

Earlier work [17] on the calculation of the heat demand of batch melting yielded considerable success for batches with a small number of chemically pure raw materials. The former calculation strategy was based on the formulation of a gap-less sequence of chemical and physical reactions linking the stage of batch at 25 °C to the stage of glass melt at a given temperature. For a realistic industrial batch, this is virtually impossible to accomplish. Beyond this, the strategy gives up a noble principle of thermodynamics, i.e., the path independence of the properties of thermodynamic states. With the successful thermodynamic quantification of the states of industrial glasses and glass melts (sections 1.1 and 1.2), we may fully exploit the principle of path independence and present the batch-to-melt conversion by the hypothetical reaction, given in eq. (2).

The energy difference between the right and left hand side of eq. (2) is the standard heat of formation of glass and batch gases from the raw materials,  $\Delta H^\circ_{\text{chem}}$ , also termed chemical heat demand of batch melting.  $\Delta H^\circ_{\text{chem}}$  is calculated as

$$\Delta H^\circ_{\text{chem}} = H^\circ_{\text{glass}} + H^\circ_{\text{gas}} - H^\circ_{\text{batch}} \quad , \quad (9)$$

where  $H^\circ_{\text{glass}}$  is determined after eq. (7 a), and  $H^\circ_{\text{gas}}$ ,  $H^\circ_{\text{batch}}$  are the weighted sums of standard heats of the individual batch gases and raw materials, respectively. For simple batches containing chemically pure raw materials, eq. (9) may be evaluated in a straight-forward way.

Table 5 summarizes earlier calorimetric results [18] on the standard heats of formation of Na<sub>2</sub>O-CaO-SiO<sub>2</sub> glasses from the pure raw materials quartz, calcite and soda ash. The calculated values are obtained by characterizing the glasses as described before. The good agreement between calculation and experiment shows that additional mixing terms can be neglected even in these sodia rich systems.

Note that for the above scientific rather than technical glass compositions, the true equilibrium phases N<sub>3</sub>S<sub>8</sub> and NCS<sub>5</sub> (see [19], no. 5321) were taken into account as normative phases of the c.r.s.. These phases, however, are identified in very pure systems and under very slow cooling only. Otherwise, the metastable substitutes NS<sub>2</sub> and NC<sub>3</sub>S<sub>6</sub> are formed. Therefore, for industrial soda-lime based mass glasses, the oxides Na<sub>2</sub>O, CaO, and SiO<sub>2</sub> are always allotted to the normative phases NS<sub>2</sub>, NC<sub>3</sub>S<sub>6</sub>, and S. Since this important class of glass composition stems from a narrow composition range only, the solution of eq. (6 a-c) can be presented in a straight-forward way by

$$\begin{aligned} \text{NAS}_6 &= 5.1440 \cdot \text{Al}_2\text{O}_3 - 5.5697 \cdot \text{K}_2\text{O} \\ \text{KAS}_6 &= 5.9102 \cdot \text{K}_2\text{O} \\ \text{Hm} &= 0.6 \cdot \text{Fe}_2\text{O}_3 \\ \text{FS} &= 0.7345 \cdot \text{Fe}_2\text{O}_3 \\ \text{MS} &= 2.4907 \cdot \text{MgO} \\ \text{NC}_3\text{S}_6 &= 3.5112 \cdot \text{CaO} \\ \text{NS}_2 &= 2.9386 \cdot \text{Na}_2\text{O} + 1.9346 \cdot \text{K}_2\text{O} - 1.7867 \cdot \text{Al}_2\text{O}_3 - 1.0824 \cdot \text{CaO} \\ \text{S} &= \text{rest to the total mass.} \end{aligned}$$

All quantities are given in mass amounts; neutral redox conditions of the melt are assumed.

Until now, we have been approximating the raw materials by pure chemical substances. This may look like an acceptable simplification. But the contrary is the case: The formation data of some natural raw materials deviate from those of their chemically pure counterparts in a considerable way. In principle, each of such raw materials represents an individual multi-component minerals system of its own and has to be treated this way. For different feldspar and sand qualities, the standard enthalpies in units of kJ/g are directly found from

$$H^\circ = 15.174 \cdot \text{SiO}_2 + 17.100 \cdot \text{Al}_2\text{O}_3 + 4.633 \cdot \text{Fe}_2\text{O}_3 + 15.030 \cdot \text{MgO} + 12.035 \cdot \text{CaO} \\ + 10.52 \cdot \text{Na}_2\text{O} + 7.639 \cdot \text{K}_2\text{O},$$

which is again an easy and straight-forward solution of eqs. (6 a-c) for the narrow compositional range typical of these minerals. The oxide amounts have to be inserted in g per 100 g of the mineral. Other natural raw materials require more attention. In the following section, glass grade dolomites and limestones are treated as examples.

### 3.2 Dolomite and limestone as examples of complex raw materials

Dolomites and limestones are the minerals typically used as carriers of MgO and CaO. They are added to the batch as carbonates, or alternatively, in their partially or fully calcined form as “dolime” MgO + CaCO<sub>3</sub> or as burnt dolomite MgO + CaO and burnt lime CaO, respectively. The decomposition of alkaline earth carbonates makes the largest contribution to the chemical heat demand of the batch-to-melt conversion. Thus, from the point of view of on-site production efficiency, it may be advisable to use partially or fully calcined products in the batch. In order to assess an accurate value for  $\Delta H^\circ_{\text{chem}}$ , reliable data on the energetic situation of limestone and dolomite are required. When, however, inspecting literature data, there is a striking uncertainty, especially with respect to the heats of formation of dolomite. This issue deserves a closer look.

In table 6, heats of formation of dolomite from the elements as taken from several renowned data bases are contrasted. The uncertainty amounts to 30 kJ/mol, which is equivalent to 163 kJ per kg dolomite or 311 kJ per kg MgO + CaO equivalent.

From the point of view of mineralogy, natural dolomite and limestone are no pure phases, but rather minerals from the system CaCO<sub>3</sub>-MgCO<sub>3</sub>-FeCO<sub>3</sub>-MnCO<sub>3</sub>, accompanied by minor amounts of quartz, olivine, and feldspatic minerals. They display a most complex polycrystalline microstructure of coexisting carbonates, even in the individual grains, ranging from coarse to fine and crypto-crystalline phases. Figure 3 illustrates the phase relations in the ternary sub-system CaCO<sub>3</sub>-CaMg(CO<sub>3</sub>)<sub>2</sub>-CaFe(CO<sub>3</sub>)<sub>2</sub>, redesigned after data from [19], nos. 2753 and 4664. According to figure 3, calcite may dissolve considerable amounts of Mg. By contrast, dolomite may dissolve much Fe (such a dolomite would not be used in glass industry), however, hardly any excess Ca. Thus, a natural glass-grade dolomite always contains at least two kinds of phases, i.e., Mg saturated limestone and Ca saturated dolomite.

A very careful study [24-26] may help to resolve the discrepancies found in table 6. As can be expected from figure 3, even small amounts of Ca excess in dolomite considerably shift the resulting heat of formation of the mineral. The Fe vs. Mg

substitution yields less strong effects. The smallest shift is observed for Mg excess in pure limestone. Let us consider the heat of formation of  $\text{Ca}_{1+x}(\text{Fe}_{(1-x)}\text{Mg}_{(1-x)(1-y)})(\text{CO}_3)_2$ . For  $x = 1$ , the formula denotes pure  $\text{Ca}_2(\text{CO}_3)_2$ , for  $x = 0$ ,  $\text{Ca}(\text{Fe}_y\text{Mg}_{1-y})(\text{CO}_3)_2$  with pure dolomite and pure ankerite as end members ( $y = 0$  and  $1$ , respectively). Then, based on the results by [24-26], the standard enthalpies of formation, given in units of kJ per mol of formula unit, are calculated from the chemical composition as

$$H_{\text{dolo}}^{\circ} = -2314.2 + 129.4 \cdot x + 74.0 \cdot y \quad (9)$$

for the one-phase dolomite solid solution and

$$H_{\text{lime}}^{\circ} = -2413.8 - 9.97 \cdot (1 - x) \quad (10)$$

for the one-phase limestone solid solution. The stoichiometric coefficients  $x$  and  $y$  are derived from the analytically determined mass ratios  $u = \text{MgO}/\text{CaO}$  and  $v = \text{FeO}/\text{MgO}$  as

$$x = (0.7188 - u)/(0.7188 + u) \quad (11 \text{ a})$$

$$y = v/(1.7832 + v) \quad (11 \text{ b})$$

with the figures 0.7188 and 1.7832 representing the molar mass ratios of MgO/CaO and FeO/MgO, respectively. Thus, the standard enthalpy of a natural dolomite and limestone can be swiftly calculated from analytical data.

### 3.3 Modeling the batch-to-melt conversion

With the principles explained in sections 3.1 and 3.2, we may now complete our task and determine the chemical part  $\Delta H^{\circ}_{\text{chem}}$  of the exploited heat  $H_{\text{ex}}$ , eq. (1). In table 7, the calculation procedure is demonstrated for two different batches – batch 1 using dolomite and limestone, batch 2 using fully burnt dolomite and lime – yielding a glass identical with our reference E glass (see table 2). The values of  $\Delta H^{\circ}_{\text{chem}}$  for both batches differ considerably.

When glass cullets are added to the batch – which is standard industrial practice, then the chemical contribution to  $H_{\text{ex}}$  is reduced to  $(1 - y_C) \cdot \Delta H^{\circ}_{\text{chem}}$ , where  $y_C$  denotes the mass fraction of cullets referred to the total mass of produced glass. With  $y_C = 0.2$  and a value of 454.6 kWh/t for  $\Delta H_{\text{melt}}$  at  $T_{\text{ex}} = 1300 \text{ }^{\circ}\text{C}$ , the exploited heat for the two batches in table 7 amounts to 660 and 509 kWh per t of produced glass, respectively.

$H_{\text{ex}}$  is an integral quantity referring to the entire melting process. The principles elaborated before can also be used to give an approximate image of the reaction path itself.

This is demonstrated in table 8 for a simple soda lime silicate glass batch. The path starts from the batch at  $25 \text{ }^{\circ}\text{C}$  and passes through milestone states reached at arbitrarily selected temperatures. These are: the melting temperature of the soda ash

(860 °C) as the temperature of primary melt formation, the decomposition temperature of the limestone (900 °C), the liquidus temperature of the glass melt (960 °C), plus two process temperatures (the maximum temperature in the basin, 1400 °C, and the pull temperature  $T_{ex}= 1200$  °C). The heat balance is given in terms of the enthalpy difference  $\Delta H$  to the initial state. Thus, the  $\Delta H$  in the last column is identical with the chemical heat demand  $\Delta H^{\circ}_{chem}$ . As a special feature, the viscosity of the melt is calculated for every state. It is interesting to note that, in spite of a steady increase of temperature from 860 to 1400 °C, the viscosity does not decrease steadily, but rather passes through minima and maxima. Simultaneously, the mass fraction  $y_{solid}$  of solid matter in the melt decreases steadily. In soda lime glass batches, silica is usually the phase dissolving last.

Finally, it is demonstrated what additional information may be gained by employing a sophisticated commercial programme and database like FACTSAGE [7]. Surprisingly enough, some of these programmes do not make any use of the well established experimental experience of phase coexistence at 298 K, but rather have the ambition to calculate such phase coexistence relations at 298 K from the fundamental thermodynamic data of individual phases. This makes it especially difficult to describe multicomponent frozen-in phases (i.e., glasses) at 298 K. On the other hand, such concepts enfold their strengthes in presenting partially crystalline equilibrium stages in the range from the appearance of the first liquid phase towards complete melting. Figure 4 gives an example, again referring to the E glass composition given in table 2 and to batch no. 1 in table 7. The technologically most relevant liquidus temperature of the E glass is determined as 1245 °C; the corresponding primary phase is anorthite. Another most significant temperature level is the temperature at which solid silica disappears (1150 °C). Thus, for this E glass batch, the sand grains may dissolve via chemical driving forces even before the liquidus of the system is reached. At this point, the melt has a composition (by wt.) of 56.9 SiO<sub>2</sub>, 11.9 Al<sub>2</sub>O<sub>3</sub>, 7.7 B<sub>2</sub>O<sub>3</sub>, 0.49 Fe<sub>2</sub>O<sub>3</sub>, 4.74 MgO, 17.56 CaO, 0.69 Na<sub>2</sub>O and a viscosity of 10<sup>3.27</sup> dPas. Let us also discuss what happens when such a batch is heated up under industrial non-equilibrium conditions: The hydrous boron carriers dehydrate well below 200 °C, which is only slightly above the equilibrium decomposition temperatures. A primary molten phase in the batch occurs at the melting point of B<sub>2</sub>O<sub>3</sub> (450 °C) at the latest. In the presence of limestone and dolomite, however, this melt may be resorbed to form solid Mg-Ca borates. So the batch may remain a granular bulk solid even until the liquidus temperature of the system. This unfavorable behavior is well known for E glass batches. As a consequence, information on a reaction path cannot be drawn from equilibrium data without hesitation. Nevertheless, the determination of the liquidus temperature alone makes it worthwhile performing such calculations.

#### 4. CONCLUSION

The author hopes that the present article encourages glass technologists to make increasing use of thermodynamic calculations to optimize their processes. In the present paper, only one – however important – issue was elaborated. This is the accurate determination of the heat involved in the glass melting process. Many other useful tasks can also be accomplished by using thermodynamic calculations. This is, e.g., the quantitative description and potential optimization of:

- the fining and refining process,
- evaporation processes from the melt,
- corrosion processes between melt and refractories, or between vapors above the melt and refractories,

which, no doubt, altogether are of high relevance to every glass technologist.

## REFERENCES

- [1] Richet, P., Bottinga, Y.: Rheology and configurational entropy of silicate melts. *Reviews in Mineralogy*, Vol. 32 (1995), 6593.
- [2] Pelton, A.D., Blander, M.: Thermodynamic analysis of ordered liquid solutions by a modified quasi-chemical approach – application to silicate slags. *Met. Trans. B*, 17 B (1986) 805-815.
- [3] Gaye, H. in: Gay, H., Colombet, D., eds., *Données thermochimiques et cinétiques relatives à certains matériaux sidérurgiques*. Commission de la Communautés Européennes Convention CEEC No. 7210-CF/301 TCM-RE 1064, Bruxelles 1984.
- [4] Bonnel, D.W., Hastie, J.W.: Ideal mixing of complex components. *High Temp. Sci.* 26 (1990) 313-334.
- [5] Shakhmatkin, B.A., Vedishcheva, N.M., Schultz, M.M. and Wright, A.C.: The thermodynamic properties of oxide glasses and glass forming liquids and their chemical structure. *J. Non-Cryst. Solids* 177 (1994), pp. 249 – 256.
- [6] Eriksson, G., Hack, K.: ChemSage – A computer program for the calculation of complex chemical equilibria. *Met. Trans. B*, 21 B (1990) 1013.
- [7] FACTSAGE Software Ver. 5.2; Thermfact Montreal and GTT Technologies Aachen, 2004.
- [8] Conradt, R.: Thermochemistry and structure of oxide glasses. In: *Analysis of the Composition and Structure of Glass and Glass Ceramics*, H. Bach, D. Krause, eds., Springer Verlag, Berlin 1999, pp. 232 - 254.
- [9] Conradt, R.: Modeling of the thermochemical properties of multicomponent oxide melts. *Z. Metallkunde* 92 (2001), 1158-1162.
- [10] Conradt, R.: Chemical structure, medium range order, and crystalline reference state of multicomponent liquids and glasses. *J. Non-Cryst. Solids* 345&346 (2004), 16-23.
- [11] Philpotts, A. T.: Principles of igneous and metamorphic petrology. Prentice Hall, Englewood Cliffs 1990.
- [12] Seward, T.P. (principal investigator): Modeling of glass making processes for improved efficiency. High temperature glass melt property database for modeling. Work conducted under U.S. DOE grant no. DE-FG07-96EE41262. Alfred University 2003.
- [13] Richet, P.: Private communication (2004).
- [14] Schwiete, H.E., Ziegler, G.: Beitrag zur spezifischen Wärme der Gläser. (Contribution to specific heat of glasses). *Glastech. Ber.* 28 (1955), 137-146.
- [15] Moore, J., Sharp, D.E.: Note on calculation of effect of temperature and composition on specific heat of glass. *J. Am. Ceram. Soc.* 41 (1958), 461-463.
- [16] Gudovich, O.D., Primenko, V.I.: Calculation of the thermal capacity of silicate glasses and melts. *Soc. J. Glass Phys. Chem.* 11 (1985), 206-211.
- [17] Kröger, C.: Theoretischer Wärmebedarf der Glasschmelzprozesse. (Theoretical heat demand of the glass melting processes). *Glastech. Ber.* 26 (1953), 202-214.
- [18] Kröger, C.; Kreitlow, G.: Heats of solution and formation of silicates of sodium and calcium. *Glastech. Ber.* 29 (1956), pp. 393-400.
- [19] Phase Equilibria Diagrams. CD-ROM Database, Version 2.1. The American Ceramic Society, Ohio, Westerville, 1998.

- [20] Kubaschewski, O., Alcock, C.B. and Spencer, P.J.: Materials Thermochemistry. Pergamon Press, London 1993.
- [21] Philpotts, A.R.: Principles of igneous and metamorphic petrology. Prentice Hall, Englewood Cliffs 1990.
- [22] Babushkin, V. I., Matveyev, G.M. and Mchedlov-Petrosyan, O.P.: Thermodynamics of silicates. Springer Verlag, Berlin 1985.
- [23] Robie, R.A., Hemingway, B.S. and Fisher, J.R.: Thermodynamic properties of minerals and related substances at 298.15 K and 1 bar ( $10^5$  Pascals) pressure and at high temperatures. Geol. Survey Bull. U.S. Gov. Printing Office, Washington 1978.
- [24] Navrotsky, A., Capobianco, C.: Enthalpies of formation of dolomite and magnesia calcites. Am. Mineralog. 72 (1987), 782-787.
- [25] Chai, L., Navrotsky, A. and Reeder, R.J.: Energetics of calcium-rich dolomite. Geochim. Cosmochim. Acta 59 (1995), 939-944.
- [26] Chai, L., Navrotsky, A.: Synthesis, characterization, and energetics of solid solution along the dolomite-ankerite join, an implication for the stability of ordered  $\text{CaFe}(\text{CO}_3)_2$ . Am. Mineralog. 81 (1996), 1141-1147.
- [27] Saxena, S.K., Chatterjee, N., Fei, Y. and Shen, G.: Thermodynamic data on oxides and silicates. Springer Verlag, Berlin 1993.
- [28] HSC Chemistry Software Ver. 3.0.; Roine, A.; Outokumpu Research Oy, Pori, Finland 2000.

Table 1. Matrix ( $\mu_{jk}$ ) for the calculation of the normative compounds k of E glasses from their oxide composition given by the amounts  $m_j$  of oxides j in kg per kg glass; the calculation proceeds like:  $m(k = \text{SiO}_2) = 1.000 \cdot m(\text{SiO}_2) + 0.752 m(\text{TiO}_2) - 0.589 \cdot m(\text{Al}_2\text{O}_3) - 1.491 \cdot m(\text{MgO}) - 1.071 \cdot m(\text{CaO}) - 4.847 \cdot m(\text{Na}_2\text{O}) - 3.189 \cdot m(\text{K}_2\text{O})$ ;  $m(k = \text{CaO} \cdot \text{TiO}_2) = 1.702 \cdot m(\text{TiO}_2)$ ; etc.

compound k =	oxide j =								
	SiO <sub>2</sub>	TiO <sub>2</sub>	Al <sub>2</sub> O <sub>3</sub>	B <sub>2</sub> O <sub>3</sub>	Fe <sub>2</sub> O <sub>3</sub>	MgO	CaO	Na <sub>2</sub> O	K <sub>2</sub> O
SiO <sub>2</sub>	1.000	0.752	-0.589	-	-	-1.491	-1.071	-4.847	-3.189
CaO·TiO <sub>2</sub>	-	1.702	-	-	-	-	-	-	-
CaO·Al <sub>2</sub> O <sub>3</sub> ·2SiO <sub>2</sub>	-	-	2.729	-	-	-	-	-4.489	-2.953
B <sub>2</sub> O <sub>3</sub>	-	-	-	1.000	-	-	-	-	-
FeO·Fe <sub>2</sub> O <sub>3</sub>	-	-	-	-	1.000	-	-	-	-
CaO·MgO·2SiO <sub>2</sub>	-	-	-	-	-	5.372	-	-	-
CaO·SiO <sub>2</sub>	-	-1.454	-1.139	-	-	-2.882	2.071	1.874	1.233
Na <sub>2</sub> O·Al <sub>2</sub> O <sub>3</sub> ·6SiO <sub>2</sub>	-	-	-	-	-	-	-	8.462	-
K <sub>2</sub> O Al <sub>2</sub> O <sub>3</sub> ·6SiO <sub>2</sub>	-	-	-	-	-	-	-	-	5.909

Table 2. Composition on a reference E glass [12] given in terms of both oxides j and normative compounds k; M = molar mass in kg/kmol; m = mass in kg per 100 kg glass; n = molar amount in kmol per 100 kg glass

oxide j	M <sub>j</sub>	m <sub>j</sub>	n <sub>j</sub>	compound k	M <sub>k</sub>	m <sub>k</sub>	n <sub>k</sub>
SiO <sub>2</sub>	60.084	55.15	0.9179	SiO <sub>2</sub>	60.084	18.77	0.3124
TiO <sub>2</sub>	79.898	0.57	0.0071	CaO·TiO <sub>2</sub>	135.977	0.97	0.0071
Al <sub>2</sub> O <sub>3</sub>	101.961	14.42	0.1414	CaO·Al <sub>2</sub> O <sub>3</sub> ·2SiO <sub>2</sub>	278.208	36.61	0.1316
B <sub>2</sub> O <sub>3</sub>	69.619	6.86	0.0985	B <sub>2</sub> O <sub>3</sub>	69.619	6.86	0.0985
Fe <sub>2</sub> O <sub>3</sub>	159.691	0.44	0.0055	FeO·Fe <sub>2</sub> O <sub>3</sub>	231.537	0.34	0.0015
FeO	71.846		0.0055	FeO·SiO <sub>2</sub>	131.930	0.15	0.0011
MgO	40.311	4.22	0.1047	CaO·MgO·2SiO <sub>2</sub>	216.558	22.67	0.1047
CaO	56.079	17.73	0.3162	CaO·SiO <sub>2</sub>	116.163	8.45	0.0728
Na <sub>2</sub> O	61.979	0.61	0.0098	Na <sub>2</sub> O·Al <sub>2</sub> O <sub>3</sub> ·6SiO <sub>2</sub>	524.444	5.16	0.0098
sum		100.00				99.98	

Table 3. Thermodynamic data of compounds k employed to represent the crystalline reference systems (c.r.s.) of industrial glasses; enthalpies H in kJ/mol, entropies S and heat capacities  $c_p$  in J/(mol·K); superscripts: ° = standard state at 298.15 K, 1 bar; <sup>vit</sup> = vitrification; subscripts: <sub>melt</sub> = liquid state; <sub>1673</sub> = 1673.15 K; origin: multiple sources

K	-H°	S°	H <sup>vit</sup>	S <sup>vit</sup>	-H <sub>1673,melt</sub>	S <sub>1673,melt</sub>	C <sub>p,melt</sub>
P <sub>2</sub> O <sub>5</sub> ·3CaO	4117.1	236.0	135.1	51.5	3417.1	898.7	324.3
P <sub>2</sub> O <sub>5</sub>	1492.0	114.4	18.2	9.5	1138.5	586.6	181.6
Fe <sub>2</sub> O <sub>3</sub>	823.4	87.4	45.2	17.2	550.2	370.3	142.3
FeO·Fe <sub>2</sub> O <sub>3</sub>	1108.8	151.0	82.8	31.4	677.8	579.9	213.4
FeO·SiO <sub>2</sub>	1196.2	92.8	36.7	13.8	962.3	342.7	139.7
2FeO·SiO <sub>2</sub>	1471.1	145.2	55.2	20.5	1118.8	512.1	240.6
MnO·SiO <sub>2</sub>	1320.9	102.5	40.2	15.1	1085.3	345.2	151.5
2ZnO·SiO <sub>2</sub>	1643.1	131.4	82.4	31.4	1261.1	494.5	174.5
ZrO <sub>2</sub> ·SiO <sub>2</sub>	2034.7	84.5	86.6	32.6	1686.2	381.2	149.4
CaO·TiO <sub>2</sub>	1660.6	93.7	67.4	25.5	1365.7	360.2	124.7
TiO <sub>2</sub>	903.7	185.4	40.2	19.7	741.0	335.6	87.9
BaO·Al <sub>2</sub> O <sub>3</sub> ·2SiO <sub>2</sub>	4222.1	236.8	130.5	95.4	3454.3	1198.3	473.2
BaO·2SiO <sub>2</sub>	2553.1	154.0	81.6	26.8	2171.1	533.5	241.4
BaO·SiO <sub>2</sub>	1618.0	104.6	56.5	41.0	1349.8	361.1	146.4
Li <sub>2</sub> O·Al <sub>2</sub> O <sub>3</sub> ·4SiO <sub>2</sub>	6036.7	308.8	184.1	12.1	5235.4	1173.2	498.7
Li <sub>2</sub> O·SiO <sub>2</sub>	1648.5	79.9	16.7	6.3	1416.7	339.7	167.4
K <sub>2</sub> O·Al <sub>2</sub> O <sub>3</sub> ·6SiO <sub>2</sub>	7914.0	439.3	106.3	29.3	6924.9	1559.4	765.7
K <sub>2</sub> O·Al <sub>2</sub> O <sub>3</sub> ·2SiO <sub>2</sub>	4217.1	266.1	80.4	22.1	3903.7	666.5	517.6
K <sub>2</sub> O·4SiO <sub>2</sub>	4315.8	265.7	26.4	21.3	3697.8	983.7	410.0
K <sub>2</sub> O·2SiO <sub>2</sub>	2508.7	190.6	12.6	23.9	2153.1	595.4	275.3
Na <sub>2</sub> O·Al <sub>2</sub> O <sub>3</sub> ·6SiO <sub>2</sub>	7841.2	420.1	125.0	28.4	6870.1	1512.5	648.1
Na <sub>2</sub> O·Al <sub>2</sub> O <sub>3</sub> ·2SiO <sub>2</sub>	4163.5	248.5	92.0	27.9	3614.1	856.9	423.8
B <sub>2</sub> O <sub>3</sub>	1273.5	54.0	18.2	11.3	1088.7	271.1	129.7
Na <sub>2</sub> O·B <sub>2</sub> O <sub>3</sub> ·4SiO <sub>2</sub>	5710.9	270.0	42.7	21.1	4988.0	1090.2	637.6
Na <sub>2</sub> O·4B <sub>2</sub> O <sub>3</sub>	5902.8	276.1	58.3	40.1	4986.7	1275.5	704.2
Na <sub>2</sub> O·2B <sub>2</sub> O <sub>3</sub>	3284.9	189.5	48.8	26.6	2735.9	780.3	444.8
Na <sub>2</sub> O·B <sub>2</sub> O <sub>3</sub>	1958.1	147.1	43.6	19.5	1585.7	538.7	292.9
2MgO·2Al <sub>2</sub> O <sub>3</sub> ·5SiO <sub>2</sub>	9113.2	407.1	135.8	41.4	7994.8	1606.2	1031.8
MgO·SiO <sub>2</sub>	1548.5	67.8	46.6	13.6	1318.0	296.2	146.4
2MgO·SiO <sub>2</sub>	2176.9	95.4	61.4	11.0	1876.1	402.9	205.0
CaO·MgO·2SiO <sub>2</sub>	3202.4	143.1	92.3	25.7	2733.4	621.7	355.6
2CaO·MgO·2SiO <sub>2</sub>	3876.9	209.2	106.7	32.0	3319.2	775.3	426.8
CaO·Al <sub>2</sub> O <sub>3</sub> ·2SiO <sub>2</sub>	4223.7	202.5	103.0	37.7	3628.8	791.2	380.7
2CaO·Al <sub>2</sub> O <sub>3</sub> ·SiO <sub>2</sub>	3989.4	198.3	129.9	49.4	3374.0	787.8	299.2
3Al <sub>2</sub> O <sub>3</sub> ·2SiO <sub>2</sub>	6820.8	274.9	188.3	71.5	5816.2	1231.8	523.4
CaO·SiO <sub>2</sub>	1635.1	83.1	49.8	18.8	1382.0	329.7	146.4
2CaO·SiO <sub>2</sub>	2328.4	120.5	101.3	38.5	1868.2	509.2	174.5
Na <sub>2</sub> O·2SiO <sub>2</sub>	2473.6	164.4	29.3	13.2	2102.5	588.7	261.1
Na <sub>2</sub> O·SiO <sub>2</sub>	1563.1	113.8	37.7	9.8	1288.3	415.1	179.1
3Na <sub>2</sub> O·8SiO <sub>2</sub> *)	9173.0	597.0	94.2	34.2	-	-	-
Na <sub>2</sub> O·3CaO·6SiO <sub>2</sub>	8363.8	461.9	77.3	20.5	7372.6	1555.6	786.6
Na <sub>2</sub> O·2CaO·3SiO <sub>2</sub>	4883.6	277.8	57.7	13.4	4240.9	990.4	470.3
2Na <sub>2</sub> O·CaO·3SiO <sub>2</sub>	4763.0	309.6	87.0	22.6	4029.6	1107.9	501.2
Na <sub>2</sub> O·CaO·5SiO <sub>2</sub> *)	5934.0	349.0	63.3	30.4	-	-	-
SiO <sub>2</sub>	908.3	43.5	6.9	4.0	809.6	157.3	86.2

\*) only relevant for chemically pure Na<sub>2</sub>O-CaO-SiO<sub>2</sub> glasses

Table 4. Heat content  $\Delta H_{T,liq}$  in kWh/t of a mineral fibre glass melt with a composition of 58.2 SiO<sub>2</sub>, 1.1 Al<sub>2</sub>O<sub>3</sub>, 3.4 Fe<sub>2</sub>O<sub>3</sub>, 9.0 MgO, 23.5 CaO, 4.6 Na<sub>2</sub>O, 0.2 K<sub>2</sub>O (wt. %) at different temperatures; calculated and experimental values (inverse drop calorimetry)

T in °C	1408	1360	1352
after Schwiete und Ziegler [14]	448	429	426
after Moore & Sharp [15]	441	424	421
after Gudovich & Primenko [16]	391	374	371
own model	465	447	444
experimental value ( $\pm 21$ )	472	445	440

Table 5. Heats of formation  $\Delta H^f$  of N-C-S glasses, N = Na<sub>2</sub>O, C = CaO, S = SiO<sub>2</sub> from pure quartz, calcite, and soda ash; calculated and experimental data; for each glass, the corner compounds of the respective constitutional sub-ranges are given

				$\Delta H^f$ in kJ per 100 g	
SiO <sub>2</sub>	CaO	Na <sub>2</sub> O	c.r.s.	calc.	exp. [18]
74.1	10.1	15.8	N <sub>3</sub> S <sub>8</sub> -NCS <sub>5</sub> -S	50.5	51.3 $\pm$ 0.8
75.3	11.7	13.0	NC <sub>3</sub> S <sub>6</sub> -NCS <sub>5</sub> -S	47.5	49.3 $\pm$ 1.0
71.0	13.8	15.3	NS <sub>2</sub> -NC <sub>3</sub> S <sub>6</sub> -NCS <sub>5</sub>	53.2	55.7 $\pm$ 1.0

Table 6. Compilation of literature data on the standard heat of formation  $H^\circ$  of dolomite from the elements; n.n. = unspecified

$H^\circ$ in kJ/mol CaMg(CO <sub>3</sub> ) <sub>2</sub>	kind	source	
-2315.0 $\pm$ 5.0	n.n.	Kubaschewski et al. 1993	[20]
-2329.9	n.n.	Philpotts 1990	[21]
-2331.7	n.n.	Mchedlov-Petrossyan 1985	[22]
-2324.5	n.n.	Robie et al. 1978	[23]
-2314.2 $\pm$ 0.5	disordered	Navrotsky et al.	[24-26]
-2300.2 $\pm$ 0.6	ordered	Navrotsky et al.	[24-26]
-2325.7	n.n.	Saxena et al. 1993	[27]
		FACT-SAGE 5.2	[7]
-2326.3	"CaCO <sub>3</sub> -MgCO <sub>3</sub> "	HSC CHEMISTRY	[28]
-2317.6	disordered	HSC CHEMISTRY	[28]
-2329.9	ordered	HSC CHEMISTRY	[28]

Table 7. Calculation of the chemical heat demand  $\Delta H^{\circ}_{\text{chem}}$  of two different batches given in amounts of kg per 1000 kg of glass, both yielding the reference E glass (see table 2); M = molar mass,  $H^{\circ}$  = standard enthalpy

	M	$H^{\circ}$	batch 1		batch 2	
	g/mol	kWh/kg	kg	kWh	kg	kWh
sand	60.084	-4.2112	-562.00	2366.7	-562.00	2366.7
Al <sub>2</sub> O <sub>3</sub>	101.961	-4.5652	-144.00	657.4	-144.00	657.4
3H <sub>2</sub> O·B <sub>2</sub> O <sub>3</sub>	123.664	-4.9152	-97.30	478.2	-97.30	478.2
Na <sub>2</sub> O·2B <sub>2</sub> O <sub>3</sub> ·5H <sub>2</sub> O	291.292	-4.5676	-28.90	132.0	-28.90	132.0
dolomite	184.410	-3.4859	-192.80	672.1	-	0.0
burnt dolomite	96.390	-3.5634	-	0.0	-100.80	359.2
limestone	100.089	-3.3495	-211.50	708.4	-	0.0
burnt lime	56.079	-3.1449	-	0.0	-118.50	372.7
I. sum of batch			-1236.50	5014.8	-1051.50	4366.2
CO <sub>2</sub>	44.010	-2.4837	185.04	-459.6	0.00	0.0
H <sub>2</sub> O	18.015	-3.7284	51.46	-191.9	51.50	-192.0
II. sum of gases			236.50	-651.4	51.50	-192.0
III: glass		-4.1065	1000.00	-4106.5	1000.00	-4106.5
$\Delta H^{\circ}_{\text{chem}} = \text{I} + \text{II} + \text{III}$				256.9		67.7

Table 8. Reaction path of a simple soda lime silicate glass batch yielding a glass of 74 SiO<sub>2</sub>, 10 CaO, 16 Na<sub>2</sub>O (by wt.); reaction path given as a function of temperature in amounts (kg per 1000 kg glass) of solid phases, CO<sub>2</sub> gas, and melt; T<sub>liq</sub> = 960 °C;

ΔH = enthalpy difference to the cold batch in kWh per 1000 kg glass; y<sub>solid</sub> = mass fraction solid/(solid + melt); η = viscosity in dPa·s

temperature in °C	25	860	900	960	1200 <sup>*)</sup>	1400	1200 <sup>#)</sup>	25
<b>solid phases</b>								
quartz l/h	740.0	740.0	-	-	-	-	-	-
limestone	178.5	178.5	178.5	-	-	-	-	-
soda ash	273.6	-	-	-	-	-	-	-
cristobalite	-	-	480.8	287.0	287.0	-	-	-
total solids	1192.1	918.5	659.3	287.0	287.0			
<b>liquid or glassy components</b>								
soda ash	-	273.6	-	-	-	-	-	-
Na <sub>2</sub> O·SiO <sub>2</sub>	-	-	103.6	-	-	-	-	-
Na <sub>2</sub> O·2SiO <sub>2</sub>	-	-	315.6	361.9	361.9	361.9	361.9	361.9
Na <sub>2</sub> O·3CaO·6SiO <sub>2</sub>	-	-	-	351.1	351.1	351.1	351.1	351.1
SiO <sub>2</sub>	-	-	-	-	-	287.0	287.0	287.0
total melt	-	273.6	419.2	713.0	713.0	1000.0	1000.0	1000.0
<b>batch gases</b>								
CO <sub>2</sub>	-	-	113.6	192.1	192.1	192.1	192.1	192.1
<b>heat, content of dispersed solids, viscosity of liquid phase</b>								
ΔH in kWh	0	350	431	471	585	681	589	134
y <sub>solid</sub>	1.00	0.77	0.66	0.29	0.29	0	0	0
log η(melt)	-	-2.0	1.9	4.3	1.8	2.1	2.8	-

\*) under equilibrium conditions, the amount of solid phases at T > T<sub>liq</sub> is zero; in the industrial process, however, the residual silica dissolves at a considerable rate only if log η < 2 – 3

#) pull temperature T<sub>ex</sub>

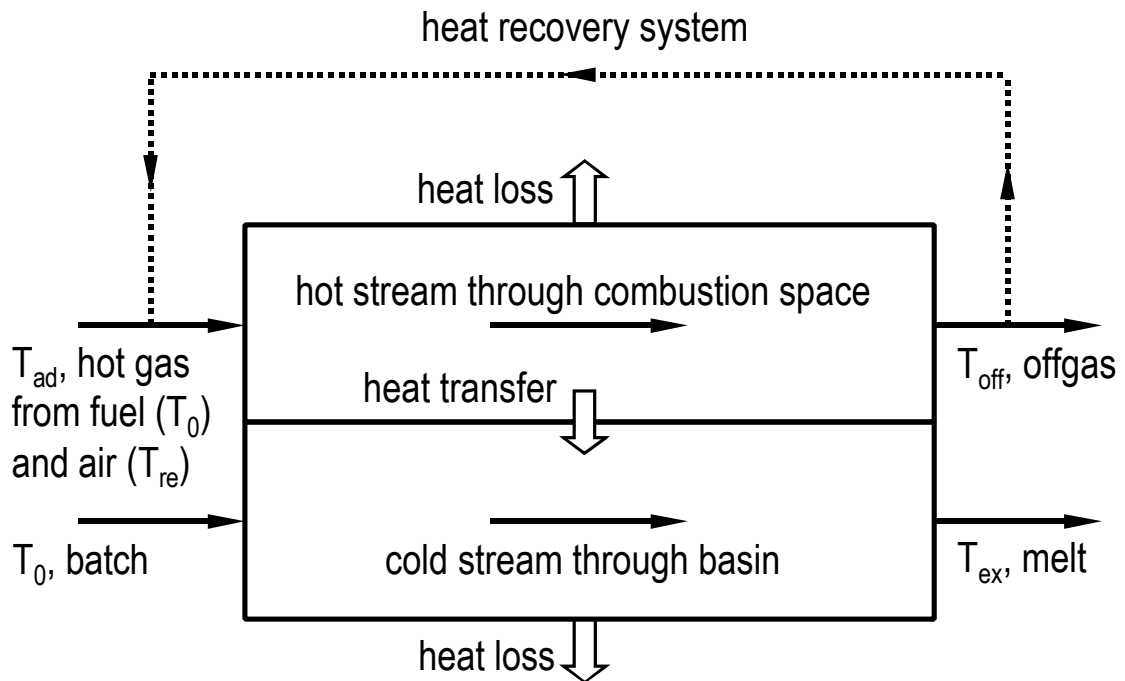


Fig. 1. Sketch of the principle function of a continuously working glass melting tank furnace;  $T_0$  = ambient temperature,  $T_{re}$  = temperature of pre-heated air,  $T_{ad}$  = adiabatic combustion temperature,  $T_{off}$  = offgas temperature,  $T_{ex}$  = pull temperature of the glass melt

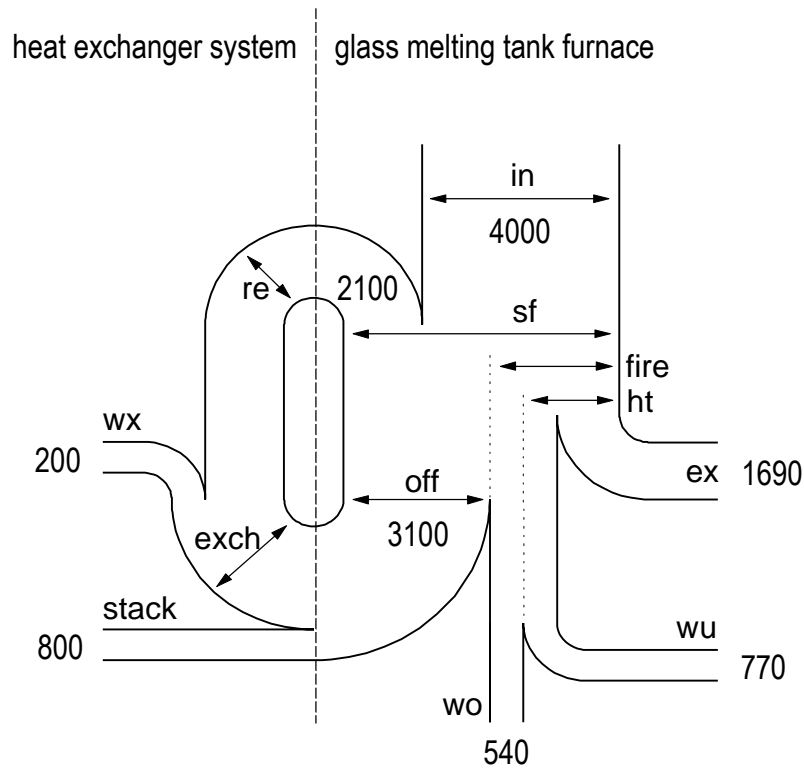


Fig. 2. Heat balance of a continuously working glass melting tank furnace; typical figures of the individual heat terms given in kJ per kg of molten glass; abbreviations denoting individual heat terms:

- in: heat input by fuel and electricity,
- sf: heat set free in the furnace,
- fire: heat transferred to the furnace body,
- ht: heat transferred to the basin,
- ex: exploited heat,
- off: heat stored in the offgas leaving the furnace,
- stack: heat stored in the offgas leaving the heat exchanger,
- exch: heat transferred to the body of the heat exchanger,
- re: heat recovered by the air passing through the heat exchanger,
- wu: wall losses through the basin,
- wo: wall losses through the lining of the combustion space,
- wx: wall losses of the heat exchanger

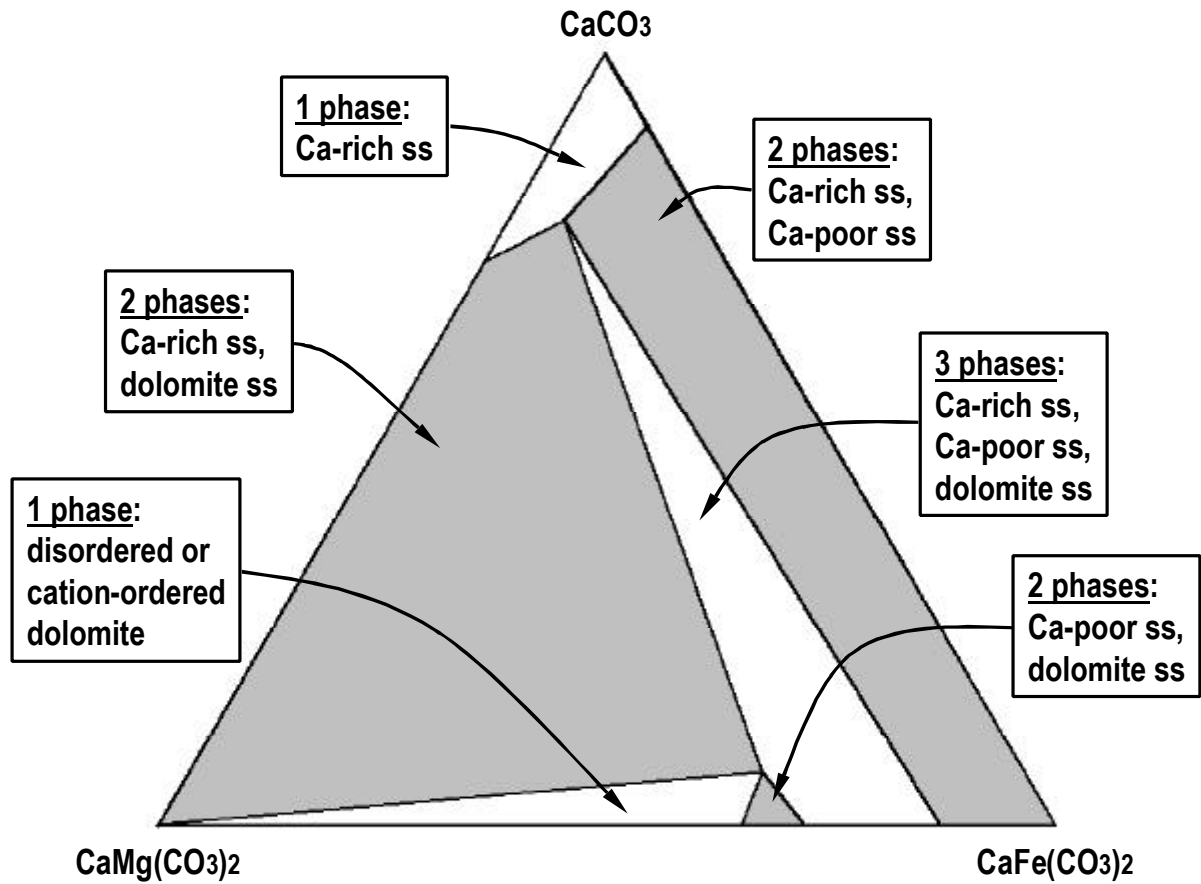


Fig. 3. Phase diagram of the system  $\text{CaCO}_3\text{-CaMg}(\text{CO}_3)_2\text{-CaFe}(\text{CO}_3)_2$  showing the stability fields of one-, two-, and three-phase equilibria

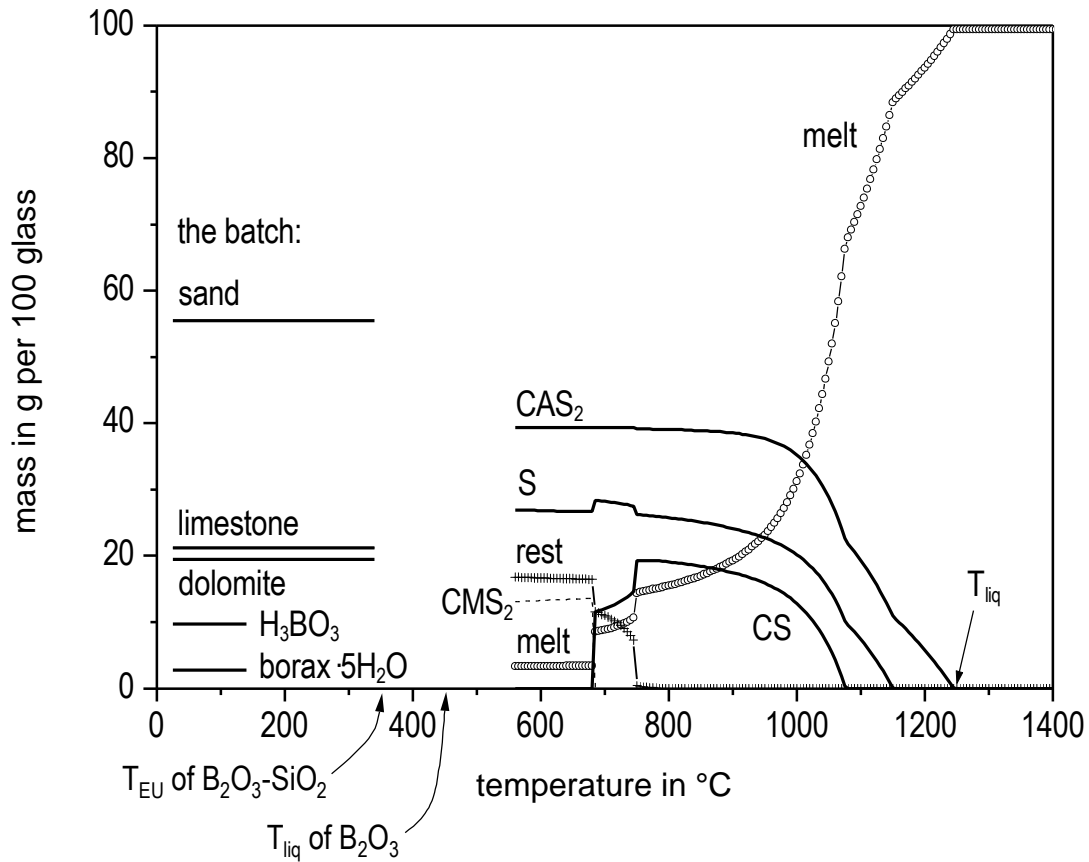


Fig. 4. Phase coexistence in the E glass batch no.1 shown in table 7 as a function of temperature; the hydrous boron carriers dehydrate well below 200 °C; a primary molten phase occurs between 350 and 450 °C; under industrial non-equilibrium conditions, this melt is absorbed by the limestone and dolomite to form solid Ca-Mg borates, and the batch may remain „dry“ even until T<sub>liq</sub>